Annu. Rev. Microbiol. 2004. 58:233–51
doi: 10.1146/annurev.micro.58.030603.123822

First published online as a Review in Advance on May 14, 2004

RIBOSOMAL CRYSTALLOGRAPHY: Initiation, Peptide Bond Formation, and Amino Acid Polymerization are Hampered by Antibiotics

Ada Yonath[1,2] and Anat Bashan[1]
[1]*Department of Structural Biology, The Weizmann Institute, 76100 Rehovot, Israel; email: ada.yonath@weizmann.ac.il; anat.bashan@weizmann.ac.il*
[2]*Max-Planck-Research Unit for Ribosomal Structure, 22603 Hamburg, Germany*

Key Words ribosomes, initiation factor 3, exit tunnel, gating, peptidyl-transferase, synergism

■ **Abstract** High-resolution structures of ribosomal complexes revealed that minute amounts of clinically relevant antibiotics hamper protein biosynthesis by limiting ribosomal mobility or perturbing its elaborate architecture, designed for navigating and controlling peptide bond formation and continuous amino acid polymerization. To accomplish this, the ribosome contributes positional rather than chemical catalysis, provides remote interactions governing accurate substrate alignment within the flexible peptidyl-transferase center (PTC) pocket, and ensures nascent-protein chirality through spatial limitations. Peptide bond formation is concurrent with aminoacylated-tRNA 3′ end translocation and is performed by a rotatory motion around the axis of a sizable ribosomal symmetry-related region, which is located around the PTC in all known crystal structures. Guided by ribosomal-RNA scaffold along an exact pattern, the rotatory motion results in stereochemistry that is optimal for peptide bond formation and for nascent protein entrance into the exit tunnel, the main target of antibiotics targeting ribosomes. By connecting the PTC, the decoding center, and the tRNA entrance and exit regions, the symmetry-related region can transfer intraribosomal signals, guaranteeing smooth processivity of amino acid polymerization.

CONTENTS

INTRODUCTION 234
INITIATION OF THE TRANSLATION PROCESS 235
Initiation Factor 3: A Flexible Protein Factor 235
Edeine: An Antibiotic Interfering with Initiation by Limiting the Platform Mobility 237
PEPTIDE BOND FORMATION AND AMINO ACID POLYMERIZATION 238
The PTC and Its Vicinity: A Sizable Symmetry-Related Region 238
Clinically Relevant PTC Targeting 240
Sparsomycin, Puromycin, and the "Fragment Reaction" 241

POST PEPTIDE BOND FORMATION 243
Macrolides and Ketolides: Resistance and Selectivity 243
Tunnel Mobility and Ribosomal Involvement in Cellular Regulation 246

INTRODUCTION

Ribosomes are the universal cellular riboprotein assemblies that catalyze amino acid polymerization into proteins. In this process, called protein biosynthesis, the ribosomes interact with the cellular environment, select the genetic frame to be translated, form the peptide bonds, and act as polymerases to ensure smooth and efficient elongation of the newly born protein chains. The ribosomes are composed of two riboprotein subunits of unequal size that associate upon the initiation of the process and dissociate at its termination. Protein biosynthesis is performed by a cooperative effort of both subunits, and the ribosome possesses features that facilitate transmission between its various functional sites, leading to efficient processivity of protein formation essential for cell vitality. The small ribosomal subunit facilitates the initiation of the translation process and is involved in selecting the frame to be translated, decoding the genetic message, and controlling the fidelity of codon-anticodon interactions. The large ribosomal subunit forms the peptide bond, ensures smooth amino acid polymerization, and channels the nascent proteins through their exit tunnel.

Messenger RNA (mRNA) carries the genetic instructions to the ribosome, and aminoacylated transfer RNA (tRNA) molecules deliver the amino acids within a ternary complex containing GTP and the elongation factor Tu. The ribosome possesses three tRNA binding sites. The A-site hosts the aminoacylated-tRNA, the P-site hosts the peptidyl tRNA, and the E-site designates the location of the exiting free tRNA once a peptide bond has been formed. Elongation of the polypeptide chain is driven by GTPase activity. This motion is associated with A $\rightarrow$ P $\rightarrow$ E translocation of the mRNA together with the tRNA molecules bound to it. In each step of the elongation event, the mRNA advances by one codon and a new peptide bond is formed between the amino acid bound to the A-site tRNA and the growing peptidyl bound to the P-site tRNA. The leaving group of this reaction, a free tRNA molecule, is released from the ribosome through the E-site as a part of the overall mRNA-tRNA translocation. The entire cycle of elongation is extremely fast, requiring about 50 ms for its completion from the stage of tRNA selection by the mRNA until the leaving group is released. Peptide bond formation consumes a very small portion of this time.

Two decades (84) of crystallographic attempts yielded several three-dimensional structures of free and complexed ribosomal particles, despite the common belief that ribosomal particles cannot crystallize owing to their instability, complexity, and conformational variability. The key to obtaining crystals was the use of ribosomes from robust bacteria, namely halophiles and thermophiles (79). These yielded suitable crystals from the large subunit from *Haloarcula marismortui*,

H50S (36, 61, 74), and the small subunit from *Thermus thermophilus*, T30S (82). However, because *H. marismortui* is an archaeon sharing properties with prokaryotes as well as eukaryotes, the structural information obtained from its crystals is only partially relevant to the vast amount of functional knowledge accumulated over the years from the *Escherichia coli* ribosome. The addition of a new crystal type, from the large ribosomal subunit from the robust mesophilic eubacterium *Deinococcus radiodurans*, D50S (28), the ribosomes of which have a sequence almost identical to that of *E. coli* ribosomes, addressed this need successfully.

Importantly, D50S crystallizes under conditions similar to those optimized for its maximal functional activity, and its crystals yielded functionally meaningful, well-ordered structures in contrast to the disorder of the functionally relevant features observed in the structure of H50S (4, 46). Furthermore, typical of eubacteria, *D. radiodurans* is a suitable pathogen model for antibiotics targeting the ribosome (3, 7, 8, 27, 56, 58). A central element of the cell cycle, the ribosome is one of the main targets for a broad range of antibiotics structurally diverse in nature that inhibit different ribosomal functions. Because of its huge size, the ribosome offers, theoretically, numerous different binding sites. Nevertheless, the crystal structures of more than a dozen complexes of antibiotics bound to D50S show that practically all the known drugs utilize a single or very few binding sites composed mainly of ribosomal RNA (rRNA) (3, 7, 8, 10, 11, 24, 25, 27, 48, 56, 58).

We describe how the striking ribosomal architecture, designed for smooth peptide bond formation and efficient amino acid polymerization, becomes useless by minute amounts of clinically relevant antibiotics. This article is based on the high-resolution structures of T30S (57) and D50S (28) as well as their complexes with substrate analogs (1, 2, 5, 6, 80, 81), nonribosomal factors (48), and various antibiotics targeting the ribosome (3, 7, 8, 27, 48, 56, 58). The functional analysis presented here was aided by docking onto these structures the tRNA molecules using the 5.5 Å crystal structure of their complex with *T. thermophilus* ribosome T70S (85).

For assessing the medicinal relevance of the antibiotic modes of action as revealed in their complexes with D50S, their binding sites were correlated with biochemical, genetic, and functional results (3, 62, 72, 75). Antibiotics selectivity was assessed by comparing the structural information obtained from complexes of D50S (3, 7, 8, 27, 56, 58), which resembles pathogens, with that of H50S, since the latter share properties also with eukaryotes (24, 25).

INITIATION OF THE TRANSLATION PROCESS

Initiation Factor 3: A Flexible Protein Factor

The initiation of protein biosynthesis has an important role in governing the accurate setting of the reading frame. In prokaryotes the initiation complex contains the small subunit, mRNA, three initiation factors (IF1, IF2, and IF3), and initiator

tRNA. IF3 binds strongly to the 30S subunit. It plays multiple roles in the formation of the initiation complex. It influences the binding of the other factors, acts as a fidelity factor by destabilizing noncanonical codon-anticodon interactions, selects the first mRNA codon, discriminates against leaderless mRNA chains, and acts as an antiassociation factor because it binds with high affinity to the 30S subunit and shifts the dissociation equilibrium of the 70S ribosome toward free subunits, thus maintaining a pool of 30S (23, 47). IF3 is a small, basic protein built of C- and N-terminal domains (IF3C and IF3N, respectively) connected by a rather long lysine-rich flexible linker region (Figure 1*a*). IF3C participates in most of the IF3 functional tasks, except for discrimination against noncognate tRNA, which is performed by IF3N.

The initiation complex contains the small ribosomal subunit, initiation factors, mRNA, and the first tRNA. The tRNAs are large L-shaped molecules built primarily of double helices (Figure 1*a*), but their two functional tasks reside on short single strands. The anticodon stem loop decodes the genetic information by base pairing with the mRNA on the small subunit. The tRNA acceptor stem and the universal tRNA 3′ end—composed in all tRNAs of three nucleotides, CCA, which binds the amino acid to be incorporated into the growing protein (at the A-site) and the newly formed polypeptide chain (at the P-site)—interact with the large subunit (Figure 1*a*). The initiator mRNA in prokaryotes includes an upstream purine-rich sequence, called Shine-Dalgarno (SD), that pairs with a complementary region at the 3′ end of the 16S rRNA, thus anchoring the mRNA chain. Different positions for the anti-SD region were observed in the two high-resolution structures of T30S. In the 30S functionally activated conformation (57) the SD region is located on the solvent side of the platform, whereas in the nontreated structure (78) the anti-SD region was observed in the decoding region on the 30S front face acting as an mRNA mimic, thus indicating clearly that this rather large structural element can undergo a major swing around the platform (Figure 1*b*,*c*).

IF3 was also localized in two different positions (Figure 1*d*). Cryo-electron microscopy (EM) of its complex with T30S suggested that both IF3C and IF3N are located in the interface side of the 30S subunit (39) within a region involved in extensive contacts with the 50S subunit in the entire 70S ribosome (85). In this position the location of IF3C is consistent with results of hydroxyl radical cleavage data (12) and provides a direct explanation for the role of IF3 in preventing subunit association. However, it does not address the detachment of the SD anchor, which is required for initiating the translocation process.

An alternative location for IF3C was observed in the crystal structure of a complex of T30S with IF3C (48). In this complex IF3C is located in a position that seems especially designed for it, within a cavity near the anti-SD region that matches its size and shape on the solvent side of the upper edge of the platform (Figure 1*c*). This location is consistent with results of NMR, mutagenesis, and almost all crosslinks, footprints, and protection patterns reported for *E. coli* IF3C (47), as well as with the location of the eukaryotic initiation factor 3 (eIF3), as revealed by electron microscopy in a complex of rat liver small subunit (63).

As crystals containing the entire IF3 molecule or IF3N could not be produced owing to tight crystal contacts, IF3N and IF3 linker regions were docked onto the T30S complexed with IF3C with its known crystal structures (9), taking into account the flexibility of the linker as indicated by NMR studies (19, 20). In its docked location, IF3N is positioned close to the P-site (Figure 1*a*), leaving sufficient space for cognate tRNA binding, but is too tight for allowing near-cognate or noncognate interactions (48), indicating that IF3N discriminates against noncognate tRNA by space exclusion principles. If the inherent flexibility of IF3 linker can be paralleled to that of the anti-SD region, it seems that IF3 exploits its conformational mobility for fulfilling its various tasks. It is conceivable that during the initial stages of the creation of the initiation complex, IF3 binds to the interface side of the 30S subunit, as observed by cryo-EM (39) and hydroxyl radical cleavage (12), while the linker that extends from the rim of the decoding center to the subunit solvent side acts as a strap between the two IF3 domains, presumably for transmitting signals between the two IF3 domains. Once cognate interactions are created by the initiator tRNA, namely the formation of the right initiation complex, IF3C swings to the platform backside (Figure 1*d*), facilitates the detachment of the SD region, and enables subunit association. Such IF3C swinging motion can also explain a prominent feature in the cryo-EM result (39) called the "flying object" in Figure 1*b*, which so far has not been accounted for, as this flying feature may represent a swinging IF3C domain trapped in the middle of its motion.

Edeine: An Antibiotic Interfering with Initiation by Limiting the Platform Mobility

The small ribosomal subunit seems to possess mobile elements for controlling the fidelity of the decoding process. It is built of several domains radiating from a junction located near the decoding center that seem to support correlated motions required for the protein biosynthesis process (17, 65), including the initial accommodation of the ribosomal A-site (71). Comparative studies performed on the available high-resolution structures of the free and the complexed ribosomal particles also indicate significant mobility and show that specific conformations of the small subunit can be associated with functional states and that antibiotics, such as spectinomycin, can trap the small subunit at a particular conformation (51).

A head-to-shoulder motion in the small subunit may facilitate the threading of the incoming mRNA through a dynamic pore, and the platform, located at the opposite side of the particle, is likely to perform the motions that facilitate the mRNA exit (57, 79). These motions are hindered by edeine, a universal antibiotic that inhibits the initiation of protein synthesis in all phylogenetic kingdoms. Cocrystals of edeine and T30S showed that edeine binds in the solvent side of the platform in a position that might affect the binding of IF3N, IF3 linker, and the mRNA (Figure 1*e*). It also limits the platform mobility by inducing the formation of a new base pair and physically linking the decoding site, the P-site tRNA,

and the features of the platform critical for tRNA, IF3, and mRNA binding (25). Pactamycin, an antibiotic agent that shares a protection pattern with edeine, acts in a similar fashion (10).

PEPTIDE BOND FORMATION AND AMINO ACID POLYMERIZATION

The PTC and Its Vicinity: A Sizable Symmetry-Related Region

The interface surfaces of both subunits are rich in rRNA, which comprises about two thirds of the ribosomal mass. These RNA-rich surfaces contain both ribosomal active sites, the decoding center in the small subunit and the PTC in the large subunit (Figure1*f*), thus indicating that the ribosome is a ribozyme. A flexible intersubunit bridge called B2a combines these two active sites and is composed solely of rRNA, the tip of helix H69. Its strategic location (Figure 1*f*) hints at a possible role as a platform carrying the tRNA acceptor stem from the A- to the P-site within the frame of the overall translocation process. The extension of this bridge, namely helix H69, forms part of the PTC rim. The PTC is located close to the subunit interface, at the bottom of a cavity in the large ribosomal subunit, which hosts the ribosomal protein L16 (*E. coli* numbering system is used throughout) in its upper rim (Figure 2*a*,*b*).

The ribosome is a giant asymmetric riboprotein particle. However, a large symmetry-related region containing about 180 nucleotides was revealed in all known structures of the large ribosomal subunit (Figure 2*c*) (1, 2, 5, 6), with an axis positioned close to the center of the PTC, between the A-site and the P-site loops, pointing into the protein exit tunnel (Figure 2*d–f*). This symmetry region relates the backbone fold and the nucleotides' orientations, rather than their types, and includes several nucleotides that do not obey the symmetry, mostly bulged nucleotides with functional relevance. The existence of this twofold symmetry can be justified by the need to offer comparable supportive environments to two similar chemical moieties that have to face each other to allow participation of the A-site amine and the P-site carbonyl-carbon in peptide bond formation.

In the structure of D50S in complex with ASM, a 35-ribonucleotide chain mimicking the aminoacylated-tRNA acceptor stem and its universal 3′ end (5), the ribosomal symmetry axis nearly coincides with the bond connecting the ASM double helical features to its single-stranded 3′ end, the moiety carrying the amino acid. Hence, the A-site to P-site passage is likely to involve two independent, albeit correlated, motions: a shift of the A-site tRNA helical regions, performed as a part of the overall mRNA-tRNA translocation, and a spiral rotation of the tRNA 3′ end (Figure 2*f*), consistent with results of footprinting experiments, indicating spontaneous movement of the A-tRNA acceptor stem into the P-site (77).

The outer contour of the symmetry-related region at the PTC surrounds an arched void of a size sufficient to accommodate the tRNA-3′ end, with a shape and position that seem to be designed as the path along which the rotatory motion

proceeds (Figure 2*d*,*g*,*h*). The PTC wall located away from the subunit interface, called the rear wall, forms the scaffold that guides the rotatory motion. Two universally conserved nucleotides, A2602 and U2585, that bulge into the center of the PTC from its front wall (Figure 2*d*,*f*,*g*) seem to have a pivotal role in directing the rotatory motion. A2602 is located at the upper side of the PTC, very close to the rotation axis, and can interact with the bond connecting the 3′ end and the rest of the tRNA and U2585, which resides at the bottom of the PTC and points into the ribosomal exit tunnel. The rotatory motion could be simulated with no space constraints or steric hindrances. While rotating, the A-site 3′ end slides along the backbone of two rear-wall nucleotides and may interact with the rear-wall bases that point inward. In this way the PTC walls confine the precise path for the rotating moiety, guarantee smooth A-site to P-site translocation, and ensure that the rotating moiety arrives at the P-site at a distance, configuration, orientation, and stereochemistry optimal for peptide bond formation (Figure 2*h*). Importantly, the interactions of ASM, mimicking the A-site tRNA and the derived P-site with the PTC, which represent the beginning and the end of the rotatory motion, are consistent with most of the available biochemical data (22, 32, 42, 77).

A nucleophilic attack by the amino nitrogen of the aminoacylated-tRNA can readily occur at the pH optimal for protein biosynthesis in almost all species, which is also the pH within the D50S crystals, as these are grown and maintained under close to physiological conditions (28, 79). This attack is performed while both the A-site and P-site are still occupied by the aminoacylated-tRNA and the peptidyl-tRNA, respectively, generating a tetrahedral oxyanion intermediate. The next steps of this reaction, namely $sp^3 \rightarrow sp^2$ reorganization and a transfer of a hydrogen bond to the leaving group, which leads to the deacylation of the tRNA in the P-site, seem to occur in concert with the rotatory motion. The passage of the A-site tRNA 3′ end into the P-site should assist the release of the leaving group, thus vacating the space for a new aminoacyl tRNA and securing the processivity of protein biosynthesis.

Four nucleotides of the P-site region that are located near the tunnel entrance are positioned about 2 Å lower than their A-site mates, thus acquiring a spiral nature to the rotary motion and ensuring the entrance of the nascent proteins to their exit tunnel. Hence, the rotatory motion is the key component of a unified ribosomal mechanism for peptide bond formation, translocation, and nascent protein progression. According to this integrated ribosomal machinery, the peptide bonds are formed spontaneously in an exothermic reaction that drives the elongation (1, 2, 5, 6). By providing the architectural means for accurate substrate positioning and alignment, by the design of an exact path for the A-site to P-site passage, and by the guidance of the rotatory motion along this path, the ribosome contributes positional catalysis to peptide bond formation as well as to polypeptide elongation. No ribosomal component is required for the mere chemical events of peptide bond formation, but specific ribosomal moieties may have a major influence on the rate of protein biosynthesis, which plays a key role in cell vitality (31, 52).

Elements of the PTC architecture seem to be designed for specific tasks, such as directing the initiator tRNA to the P-site. Theoretically, the first tRNA could be accommodated in the A-site or the P-site, since both are free and available. However, analyzing the potential interactions in the two PTC binding sites shows that compared with the A-site, the P-site contains an extra potential interaction that can be exploited by a tRNA 3′ end, indicating the preference for this mode of binding. Hence, the sole stereochemical requirement for extending the initiation process toward the creation of a peptide bond is that the initial P-site tRNA be at the orientation acquired at the end of the rotatory motion.

The PTC architecture also ensures the exclusive incorporation of L-amino acids and the rejection of the D-isomers, despite the occurrence of minute amounts of D-amino acids in cells. Owing to the PTC significant tolerance for substrate binding (1, 2, 5, 6, 81), one would expect that D-amino acid could be accommodated by it. Hence, the exclusivity of the L-isomer in proteins points to the existence of a ribosomal mechanism for avoiding this mistake, which should function satisfactorily despite the natural conformational flexibility of the PTC. U2506 and U2585 are the two key nucleotides responsible for D-amino acid rejection (86). Among them, U2585 is the nucleotide involved in directing the rotatory motion by interacting with the amino acid bound to the CCA, and in the placement of the first tRNA (27), consistent with the dominant lethal phenotypes produced by its mutations. Overall, the PTC exclusion of D-amino acid incorporation into the growing chain is due to space considerations as well as the creation of unproductive interactions that may be irreversible (86). Substantial conformational rearrangements within the PTC may bypass both mechanisms, consistent with the suggestion based on mutation experiments (14).

Finally, the location of the symmetry-related region suggests its participation in intraribosomal functional signaling, since it is positioned between the two lateral protuberances of the large ribosomal subunit. Both stalks possess significant conformational dynamics and are presumed to undergo cooperative motions enabling the entrance and the exit of aminoacylated and deacylated free tRNA, respectively (Figure 2*e*). Thus, the symmetry-related region connects the four most important functional sites of the ribosome: the PTC, the decoding center (via H69, located at the PTC upper rim and serving as the intersubunit bridge B2a), the GTPase center, and the L1 arm, which was suggested to serve as the "door" of the leaving tRNA molecules (2, 6, 28).

Clinically Relevant PTC Targeting

The peptidyl transferase center is a major target site for universal inhibitors produced by microorganisms as well as for clinically relevant antibiotics. Among the latter are chloramphenicol and clindamycin, which bind at the PTC and compete with A-site and P-site tRNAs (41, 53). Chloramphenicol is widely used because it is highly specific for eubacteria and has a low level of toxicity in humans. The crystal structure of D50S in complex with each of these two drugs at clinically relevant drug concentrations is consistent with these findings. Furthermore,

although their binding sites differ, the sites of these two antibiotic drugs appear to partially overlap (58).

The case of chloramphenicol is of special interest because it illuminates the differences between medically meaningful and nonrelevant binding. In the crystal structure of D50S in complex with chloramphenicol obtained at clinically relevant drug concentrations, chloramphenicol is located well within the PTC, at the A-site region. In this location (58), one of the chloramphenicol OH groups can make a hydrogen bond with G2061, a nucleotide implicated in chloramphenicol resistance in rat mitochondria (73). G2061 is also proximal to A2062, the mutation of which confers resistance in *Halobacterium halobium* (38), and to U2506, which is affected by in vivo modifications of chloramphenicol (29, 60).

Owing to the prominent selectivity of chloramphenicol, it binds to the *H. marismortui* large subunit only at extremely high concentrations, about 1000 times higher than the concentration commonly used in therapeutic treatment. Surprisingly, even these large drug amounts did not lead to chloramphenicol binding in the site that is consistent with the known biochemical and functional findings that are consistent with chloramphenicol position at the PTC. Instead, in H50S it was localized in the entrance of the ribosome tunnel, in the secondary site (25), held by contacts between its aromatic ring and the tunnel's hydrophobic crevice that hosts the common macrolides.

Sparsomycin, Puromycin, and the "Fragment Reaction"

When discovered over half a century ago, sparsomycin and puromycin were considered antibiotics because microorganisms produced them. However, owing to their universality, they are not useful clinically. Sparsomycin is a potent ribosome-targeted inhibitor that acts on all cell types. Although sparsomycin does not competitively inhibit A-site substrate binding, A-site antibiotics such as chloramphenicol compete with it for binding to bacterial ribosomes, and mutants of A-site nucleotides increase the tolerance to sparsomycin (34, 67).

Consistent with crosslink data (50), in complexes of D50S (5) and H50S (25) sparsomycin forms stacking contacts with the nucleotide A2602, positioned in the middle of the PTC. When sparsomycin is bound to an empty PTC, as in the complex D50S, it occupies the A-site side of A2602 and alters the PTC conformation, whereas when attached to the large subunit together with the P-site tRNA analog, as in its complex with H50S (25), sparsomycin points at the P-site side of this nucleotide. A2602 is a conserved nucleotide that seems to play a key role in substrate positioning, translocation, and E-site tRNA release (49). This base adopts a different orientation in each of the known complexes of the large subunit, and its striking conformational variability appears to be synchronized with the tRNA translocation within the PTC (2, 5, 6). Consequently, nucleotide A2602 was proposed to act as a conformational switch within the PTC, propelling the rotating moiety in concert with the action of helix H69, the feature that seems to assist the shift of the tRNA acceptor stem at the subunit interface (2, 6, 80, 81).

Puromycin resembles the 3′ terminus of aminoacyl-tRNA, but its aminoacyl residue is linked via an amide bridge rather than an ester bond. For over four decades it played a central role in biochemical experiments aimed at understanding the mechanism of peptide bond formation (69). Puromycin structure resembles that of the tip of aminoacylated-tRNA (Figure 2*b*); hence, it competes with A-site tRNA binding. Consequently, it was used as a part of substrate analogs designed to mimic different portions of aminoacylated-tRNA. These include compounds representing the CCA moiety, such as a tetra-oligonucleotide called ACCP (ACC-puromycin), and polynucleotides mimicking the entire portion of the tRNA that interacts with the large subunit, such as ASM (Figure 2*b*). The ends of these analogs contain puromycin, a universal ribosomal inhibitor whose structure mimics tyrosylated adenine (Figure 2*b*) (5).

A striking net of extensive interactions between the tRNA acceptor stem and the upper rim of the PTC cavity was observed in the 70S ribosome (85) as well as in complexes of D50S with tRNA acceptor stem mimics (5). These remote interactions, together with a universal base pair between the tRNA, govern the accurate positioning of the tRNA substrates (1, 2, 5, 6, 80, 81), whereas the global localization of the tRNA molecules is based on the match between the overall ribosomal architecture and the size and shape of the tRNA molecules.

Two major participants in this interaction net are protein L16 and helix H69 (Figure 2*b*). The prominent contributions of protein L16 to accurate substrate placement are reflected in the conservation of its three-dimensional structure in eubacteria and archaea, represented by D50S (28) and H50S (4), respectively, although the amino acid sequences of L16 and L10e, from the archaeon *H. marismortui*, show poor homology. Similarly, structural observations manifested the crucial contribution of H69 interactions to the key functional task of productive alignment of the tRNA substrates. Lack of remote interactions may result from the disorder of the intersubunit bridge B2a (the tip of H69), as observed for most of the functionally relevant features in the H50S high-resolution structure (Figure 2*a*) (4, 46). Similarly, tRNA analogs that are too short to reach the upper rim of the PTC cavity bind in a mode similar, albeit distinctly different, to that within the PTC (5, 26, 46, 59), requiring conformational rearrangements to participate in peptide bond formation (43).

The binding of puromycin and its derivatives to the PTC in the presence of an active donor substrate can result in peptide bond formation by a yet unknown mechanism. This so-called fragment reaction is much ($\times 10^3$) slower than the normal formation of peptide bonds (43) and can be performed under various conditions, some of which are neither similar to the optimal conditions for in vitro protein biosynthesis, nor resemble the in vivo environment. A dipeptide formed within H50S crystals by the fragment reaction, detected at the A-site, stimulated a hypothesis that this finding represents normal amino acid polymerization, which suggests that the A-site to P-site passage follows peptide bond formation (59). Such a sequence of events seems to be impractical because it implies that each time a new peptide bond is being formed, the entire newly formed polypeptide has to be rotated by 180° within the tunnel. However, because the entrance to the tunnel is

rather narrow, it poses severe space limitations, and rotations of bulky side chains may lead to significant clashes. Similarly, the alternative suggestion, that for each new peptide bond the nascent chain exploits free rotations around its main chain bonds to compensate for the 180° rotation of the tRNA 3′ end, seems to create problems because such rearrangements rule out incorporation of rigid residues, such as proline. Furthermore, postpeptide bond rotation or rearrangement should be exceedingly space and energy consuming, two assets that are hardly provided during chain elongation and may not be compensated by the only energy source of protein biosynthesis, namely the EF-G-induced GTP hydrolysis.

Thus, it seems that the attachment of this dipeptide to the A-site resulted either from improper positioning of the reactant, as observed for similar compounds in the absence of remote interactions, together with the lack of the bond around which the rotatory motion should occur; from the creation of a peptide bond under far from optimal reaction conditions [e.g., pH ∼5.6 instead of ∼8, and relatively low salt concentrations (4) instead of the high salt required for efficient protein production by *H. marismortui* (61, 79)]; or from the low affinity of puromycin derivatives to the P-site (43, 59). Peptide bond formation in the A-site within H50S crystals may reflect a special event, consistent with the variability of binding modes observed in the PTC of these crystals. Thus, five complexes of the puromycin-like substrate analogs with H50S (43) were required for reaching the conclusion that the ribosomal catalytic contribution is positional rather than chemical. Remarkably, this conclusion was evident by inspecting the structure of D50S (28) and verified by a single complex of it (5). Compared with all H50S bound analogs, the D50S complex is unique because D50S crystals are capable of providing the crucial remote interactions, as their helix H69 is well ordered (28).

The ability of the ribosome to accommodate semireactive substrate analogs, inhibitors, and compounds supposed to represent reaction intermediates (46) does not imply that each of the bound compounds could participate in amino acid polymerization, although under specific circumstances a single peptide bonds formation can be formed by the fragment reaction (59). Thus, it appears that in general the orientations of reactants that are not placed by remote interactions may be incompatible with polypeptide elongation. Furthermore, almost all substrate analogs mimicking only the tRNA 3′ end necessitated conformational rearrangement to participate in peptide bond formation and/or chain elongation (2, 6, 26, 43). Such rearrangements should require time, justifying the lower rate of the fragment reactions (43) compared with normal protein biosynthesis, and may be assisted by the PTC mobility, in which the conserved A2602 seems to play a key role by adopting various orientations (5, 6, 80, 81).

POST PEPTIDE BOND FORMATION

Macrolides and Ketolides: Resistance and Selectivity

A tunnel providing the path along which nascent proteins progress is located with its entrance adjacent to the PTC. It was first observed in the mid-1980s (40, 83) and

although inferred by biochemical experiments (37, 54), cryo-EM revisualization in the mid-1990s (16, 64) confirmed by X-ray crystallography (4, 28, 85) was required for its final recognition. This tunnel spans the large ribosomal subunit and has a nonuniform diameter. At its entrance the tunnel's diameter matches almost precisely the size of bulky amino acid residues; hence it is likely to restrict motions of large side chains as well as conformational rearrangements of rigid residues, but may allow the passage of flexible amino acid residues to which small compounds are bound (33).

This tunnel is the preferred target of a large number of antimicrobial drugs from the macrolide family, which ranks the highest in clinical usage. All macrolides studied so far bind close to the entrance of the ribosomal exit tunnel, at a distance from the PTC that permits the formation of a five- to six-amino-acid polypeptide chain before reaching the drug. All macrolides block the exit tunnel, but their binding modes and their exact positions may vary even when only one eubacterium is considered (7, 8, 27, 56, 58).

Macrolides and ketolides possess a central lactone ring, composed of 12 to 22 atoms, to which at least one sugar moiety, called desosamine, is bound (Figure 3*a*). Erythromycin, a macrolide of a 14-membered lactone ring, and its two semisynthetic derivatives, clarithromycin and roxithromycin (designed to gain stability in acidic environments and to have a broad spectrum, respectively), bind to the tunnel in a similar manner (3, 58). All three interact exclusively with rRNA, and the crystallographically observed contacts of the desosamine sugar with nucleotide A2058 (Figure *3a–c*) clarify the mechanism whereby drug resistance in clinical pathogens is acquired by A → G substitution or by the methylation of A2508 (15, 75). These interactions also clarify why the replacement of the common prokaryotic adenine by guanine, the typical eukaryotic moiety in this position, attains selectivity to 14-membered macrolides.

The rapidly acquired antibiotic resistance is a major handicap in modern medicine and stimulated the search for improved drugs. Under special conditions, 15- and 16-member macrolides developed to combat resistance bind to ribosomes with guanine in position 2058. An example is H50S, which possesses a guanine in position 2058. Therefore, in this critical aspect the archaeon *H. marismortui* resembles eukaryotes more than prokaryotes. A few macrolides belonging to the 15- and 16-member macrolide families could bind to H50S crystals when those crystals were soaked in solutions containing extremely high concentrations of antibiotics (24). However, the binding mode of azithromycin, a 15-membered ring macrolide, to the archaeal H50S differs significantly from that to the eubacterial D50S (56). In D50S azithromycin lies almost perpendicular to the tunnel long axis, similar to all other D50S complexes of clinically relevant macrolides, ketolides, and azalides studied so far. In H50S, however, the azithromycin binding mode leaves a relatively large unoccupied space within the tunnel (Figure 3*c*), thus justifying the usage of this drug for treating mammals possessing guanine in position 2058. Interestingly, in D50S complex azithromycin binds cooperatively to two sites within the exit tunnel, and similar to the ketolides ABT-773 and telithromycin, it reaches the other

side of the tunnel wall (23S RNA domain II) in addition to the typical macrolide interactions with domain V (7, 56). Thus, it seems that the recently developed ketolides and the azalides have improved pharmacokinetics and enhanced activity against certain macrolide-resistant pathogens presumably because they can form additional interactions that may compensate for the loss of the contacts with the A2058 (Figure 3*b*), which is the major site acquiring macrolide resistance.

Dual binding was observed also for streptogramins, an antibiotic family consisting of two components capable of cooperative conversion of weak bacteriostatic effects into lethal bactericidal activity. Crystals of the complex D50S-Synercid®, a recently approved injectable streptogramin with excellent synergistic activity, obtained at clinically relevant concentrations yielded the structural basis for its action (27). In this complex the Synercid S_B component binds to the same crevice of the exit tunnel that is favored by common macrolides, and interacts with the key nucleotide, A2058, in macrolide binding. Its slight inclination, compared with that of most macrolides (3, 7, 56, 58), rationalizes its reduced antibacterial effects in the absence of its S_A mate. The S_B component binds to the PTC and induces remarkable conformational alterations, including a 180° flip of U2585 base (Figure 3*g*), hence paralyzing the ability of U2585 to anchor the rotatory motion and to direct the nascent protein into the exit tunnel. When bound to D50S, both Synercid components interact with each other via the nucleotide A2062, which plays a key role in chloramphenicol (38, 58) and tylosin (24) binding. These interactions seem to stabilize the U2585 flipped conformation and consequently enhance the drug antimicrobial activity. Importantly, U2585 conformation is hardly changed in an H50S-S_A complex (25), indicating a different binding mode (Figure 3*g*) consistent with the inherent differences in PTC conformations between H50S and eubacterial ribosomes (28, 85). Similarly, the S_B interactions with A2058 in D50S explain why S_B components do not bind to H50S (25), which possesses the typical eukaryotic G rather than the common eubacterial A in this position.

An astonishing binding mode has been observed for troleandomycin (TAO), a semisynthetic derivative of erythromycin (Figure 3*a*) that has a modest clinical relevance owing to the toxicity of its metabolites. In TAO all moieties capable of participating in hydrogen bonding are either methylated or acetylated. Nevertheless, it binds close to the tunnel entrance and exploits the macrolide favorable binding site, the vicinity of A2058, albeit by making different contacts (8) (Figure 3*b*). Compared with erythromycin, TAO binds somewhat deeper in the tunnel, and its lactone ring is almost parallel to the tunnel wall and interacts not only with 23S RNA bases belonging to domain V but also with domain II. Furthermore, in contrast to other macrolides that interact exclusively with the rRNA, TAO interacts with the ribosomal protein L32.

At its unique binding orientation, TAO hits an element of the tunnel wall, the tip of protein L22 beta-hairpin, a tunnel constituent reaching from close to the PTC to the vicinity of the tunnel opening on the other side of the large subunit (28, 46). This tip consists of 11 residues and contains at its very end an amino acid triplet (*E. coli* residues 88–90) that can act as a "double hook" interacting

with the RNA, since it is composed of a highly conserved arginine, an invariant alanine, and a residue that is in most species either an arginine or a lysine. In the native large subunit structure, most of the double hook is embedded in a narrow groove so that the space available for its conformational rearrangements is rather limited. Consequently, TAO binding causes a swing of the entire L22 beta-hairpin tip across the tunnel (Figure 3*b*,*e*). As the native conformation, the resulting swung conformation is well accommodated on the tunnel walls, stabilized mainly by electrostatic interactions and hydrogen bonds (8). Importantly, the region of the tunnel wall that interacts with the L22 hairpin tip at its swung conformation seems to be designed for these extensive interactions, indicating that swinging L22 beta-hairpin tip may be a general tunnel-shaping mechanism.

Tunnel Mobility and Ribosomal Involvement in Cellular Regulation

The crystallographically observed alterations in the tunnel conformations could be correlated not only with the structures of antibiotic-resistant mutations (13, 18) but also with tunnel participation in gating and sequence discrimination (21, 30, 35, 44, 45, 55, 66, 68, 87). Examples are the SecM (secretion monitor) protein (45, 55) and the leader peptide of the *E. coli* tryptophanase (*tnaC*) operon (21). Under normal conditions, the SecM biosynthesis rate is similar to that of other proteins. The SecM protein, produced in conjunction with a protein-export system that recognizes an export signal, includes a sequence motif that causes elongation arrest in the absence of a well-functioning protein-export system. This sequence is located about 150 residues away from the protein N terminus, and within it are the main features (a proline and a tryptophan, separated by 12 residues) that trigger elongation arrest.

SecM arrest may be suppressed by mutations that can correlate remarkably (Figure 3*e*) with the tunnel regions involved in the interactions with the L22 hairpin tip at its swung conformation. It is conceivable, therefore, that the L22 hairpin tip swinging mechanism, revealed by TAO binding, represents the means by which the ribosome responds to SecM tunnel arrest signals (2, 6, 8). Protein L22 has an elongated shape and lines the tunnel wall, extending from the tunnel entrance to the vicinity of the tunnel opening (Figure 3*f*). Remarkably, this rather unusual elongated shape is maintained also in the isolated native (70) and mutated protein (13). Furthermore, in all known L22 structures a flexible region was observed only in the hairpin tip hinge region (Figure 3*f*). The efficiency of this swinging motion as a tunnel gate depends on its accuracy, which is dictated by the positioning of the L22 hinge region. A pronounced patch of positively charged amino acids, detected adjacent to the L22 hinge region (70), seems to dominate the positioning of the hinge region of the L22 hairpin stem, which in turn should enable anchoring of the double hook to both sides of the tunnel. Thus, the surface properties of L22 support a common mechanism for tunnel blockage accomplished by swinging of the L22 hairpin tip.

Within D50S a single beta-strand chain connects the protein L22 hairpin tip, and the region of this protein resides over 70 Å away, in the vicinity of the tunnel opening on the surface of the ribosome. In this location the C terminus of L22 may interact with the "pulling protein" and transmit signals according to which the swinging may be induced or eliminated by a yet unknown mechanism. The SecM nascent chain can also participate in signal transmission; after the incorporation of ~150 amino acids the chain should reach the tunnel opening. The studies showing that signal transmission through growing chains could be correlated with structural alterations in the membrane translocon pore that lines up directly with the exit tunnel (35, 87) support this suggestion.

It seems, therefore, that a swing of the L22 beta-hairpin tip, similar to that induced by TAO binding, is a universal mechanism for tunnel gating and that protein L22 is a major player in tunnel discrimination. Furthermore, protein L22 as well as the already formed portion of the nascent chain may be involved in transmitting signals from the environment into the ribosomal core. Thus, the cellular signals not only induce tunnel blockage and elongation arrest, they also control and monitor the reverse hinge motions, which are required for alleviation of the arrest by allowing sufficient space for nascent protein progression.

ACKNOWLEDGMENTS

Thanks are due to J.M. Lehn, P. Ahlberg, M. Lahav, H. Gilon, and to the ribosome groups at the Weizmann Institute, MPG for Ribosomal Structure in Hamburg and MPI Molecular Genetics in Berlin. X-ray diffraction data were collected at ID19/SBC/APS/ANL and ID14/ESRF-EMBL. The U.S. National Institutes of Health (GM34360), the German Ministry for Science & Technology (BMBF05-641EA), and the Kimmelman Center for Macromolecular Assemblies provided support. A.Y. holds the Helen and Martin Kimmel Professorial Chair.

The *Annual Review of Microbiology* is online at http://micro.annualreviews.org

LITERATURE CITED

1. Agmon I, Amit M, Auerbach T, Bashan A, Baram D, et al. 2004. Ribosomal crystallography: A flexible nucleotide anchoring tRNA translocation facilitates peptide bond formation, chirality discrimination and antibiotics synergism. *FEBS Lett.* 567:20–26
2. Agmon I, Auerbach T, Baram D, Bartels H, Bashan A, et al. 2003. On peptide bond formation, translocation, nascent protein progression and the regulatory properties of ribosomes. *Eur. J. Biochem.* 270:2543–56
3. Auerbach T, Bashan A, Harms J, Schluenzen F, Zarivach R, et al. 2002. Antibiotics targeting ribosomes: crystallographic studies. *Curr. Drug. Targets Infect. Disord.* 2:169–86
4. Ban N, Nissen P, Hansen J, Moore PB, Steitz TA. 2000. The complete atomic structure of the large ribosomal subunit at 2.4 Å resolution. *Science* 289:905–20
5. Bashan A, Agmon I, Zarivach R, Schluenzen F, Harms J, et al. 2003. Structural basis for a unified machinery of peptide bond

formation, translocation and nascent chain progression. *Mol. Cell* 11:91–102
6. Bashan A, Zarivach R, Schluenzen F, Agmon I, Harms J, et al. 2003. Ribosomal crystallography: peptide bond formation and its inhibition. *Biopolymers* 70:19–41
7. Berisio R, Harms J, Schluenzen F, Zarivach R, Hansen HAS, et al. 2003. Structural insight into the antibiotic action of telithromycin on resistant mutants. *J. Bacteriol.* 185:4276–79
8. Berisio R, Schluenzen F, Harms J, Bashan A, Auerbach T, et al. 2003. Structural insight into the role of the ribosomal tunnel in cellular regulation. *Nat. Struct. Biol.* 10:366–70
9. Biou V, Shu F, Ramakrishnan V. 1995. X-ray crystallography shows that translational initiation factor IF3 consists of two compact alpha/beta domains linked by an alpha-helix. *EMBO J.* 14:4056–64
10. Brodersen DE, Clemons WM Jr, Carter AP, Morgan-Warren RJ, Wimberly BT, Ramakrishnan V. 2000. The structural basis for the action of the antibiotics tetracycline, pactamycin, and hygromycin B on the 30S ribosomal subunit. *Cell* 103:1143–54
11. Carter AP, Clemons WM, Brodersen DE, Morgan-Warren RJ, Wimberly BT, Ramakrishnan V. 2000. Functional insights from the structure of the 30S ribosomal subunit and its interactions with antibiotics. *Nature* 407:340–48
12. Dallas A, Noller HF. 2001. Interaction of translation initiation factor 3 with the 30S ribosomal subunit. *Mol. Cell* 8:855–64
13. Davydova N, Streltsov V, Wilce M, Liljas A, Garber M. 2002. L22 ribosomal protein and effect of its mutation on ribosome resistance to erythromycin. *J. Mol. Biol.* 322:635–44
14. Dedkova LM, Fahmi NE, Golovine SY, Hecht SM. 2003. Enhanced D-amino acid incorporation into protein by modified ribosomes. *J. Am. Chem. Soc.* 125:6616–17
15. Douthwaite S, Hansen LH, Mauvais P. 2000. Macrolide-ketolide inhibition of MLS-resistant ribosomes is improved by alternative drug interaction with domain II of 23S rRNA. *Mol. Microbiol.* 36:183–93
16. Frank J, Zhu J, Penczek P, Li Y, Srivastava S, et al. 1995. A model of protein synthesis based on cryo-electron microscopy of the *E. coli* ribosome. *Nature* 376:441–44
17. Gabashvili IS, Agrawal RK, Grassucci R, Squires CL, Dahlberg AE, Frank J. 1999. Major rearrangements in the 70S ribosomal 3D structure caused by a conformational switch in 16S ribosomal RNA. *EMBO J.* 18:6501–7
18. Gabashvili IS, Gregory ST, Valle M, Grassucci R, Worbs M, et al. 2001. The polypeptide tunnel system in the ribosome and its gating in erythromycin resistance mutants of L4 and L22. *Mol. Cell* 8:181–88
19. Garcia C, Fortier PL, Blanquet S, Lallemand JY, Dardel F. 1995. 1H and 15N resonance assignments and structure of the N-terminal domain of *Escherichia coli* initiation factor 3. *Eur. J. Biochem.* 228:395–402
20. Garcia C, Fortier PL, Blanquet S, Lallemand JY, Dardel F. 1995. Solution structure of the ribosome-binding domain of *E. coli* translation initiation factor IF3. Homology with the U1A protein of the eukaryotic spliceosome. *J. Mol. Biol.* 254:247–59
21. Gong F, Yanofsky C. 2002. Instruction of translating ribosome by nascent peptide. *Science* 297:1864–67
22. Green R, Noller HF. 1997. Ribosomes and translation. *Annu. Rev. Biochem.* 66:679–716
23. Gualerzi CO, Pon CL. 1990. Initiation of mRNA translation in prokaryotes. *Biochemistry* 29:5881–89
24. Hansen JL, Ippolito JA, Ban N, Nissen P, Moore PB, Steitz TA. 2002. The structures of four macrolide antibiotics bound to the large ribosomal subunit. *Mol. Cell* 10:117–28
25. Hansen JL, Moore PB, Steitz TA. 2003. Structures of five antibiotics bound at the peptidyl transferase center of the large ribosomal subunit. *J. Mol. Biol.* 330:1061–75
26. Hansen JL, Schmeing TM, Moore PB,

Steitz TA. 2002. Structural insights into peptide bond formation. *Proc. Natl. Acad. Sci. USA* 99:11670–75
27. Harms J, Schlunzen F, Fucini P, Bartels H, Yonath A. 2004. Alterations at the peptidyl transferase centre of the ribosome induced by the synergistic action of the streptogramins dalfopristin and quinupristin. *BMC Struct. Biol.* 2:4
28. Harms J, Schluenzen F, Zarivach R, Bashan A, Gat S, et al. 2001. High resolution structure of the large ribosomal subunit from a mesophilic eubacterium. *Cell* 107:679–88
29. Izard T, Ellis J. 2000. The crystal structures of chloramphenicol phosphotransferase reveal a novel inactivation mechanism. *EMBO J.* 19:2690–700
30. Jenni S, Ban N. 2003. The chemistry of protein synthesis and voyage through the ribosomal tunnel. *Curr. Opin. Struct. Biol.* 13:212–19
31. Katunin V, Muth G, Strobel S, Wintermeyer W, Rodnina M. 2002. Important contribution to catalysis of peptide bond formation by a single ionizing group within the ribosome. *Mol. Cell* 10:339–46
32. Kim DF, Green R. 1999. Base-pairing between 23S rRNA and tRNA in the ribosomal A site. *Mol. Cell* 4:859–64
33. Kurzchalia TV, Wiedmann M, Breter H, Zimmermann W, Bauschke E, Rapoport TA. 1988. tRNA-mediated labelling of proteins with biotin. A nonradioactive method for the detection of cell-free translation products. *Eur. J. Biochem.* 172:663–68
34. Lazaro E, Rodriguez-Fonseca C, Porse B, Urena D, Garrett RA, Ballesta JP. 1996. A sparsomycin-resistant mutant of *Halobacterium salinarium* lacks a modification at nucleotide U2603 in the peptidyl transferase centre of 23 S rRNA. *J. Mol. Biol.* 261:231–38
35. Liao S, Lin J, Do H, Johnson AE. 1997. Both lumenal and cytosolic gating of the aqueous ER translocon pore are regulated from inside the ribosome during membrane protein integration. *Cell* 90:31–41
36. Makowski I, Frolow F, Saper MA, Shoham M, Wittmann HG, Yonath A. 1987. Single crystals of large ribosomal particles from *Halobacterium marismortui* diffract to 6 Å. *J. Mol. Biol.* 193:819–22
37. Malkin LI, Rich A. 1967. Partial resistance of nascent polypeptide chains to proteolytic digestion due to ribosomal shielding. *J. Mol. Biol.* 26:329–46
38. Mankin AS, Garrett RA. 1991. Chloramphenicol resistance mutations in the single 23S rRNA gene of the archaeon *Halobacterium halobium*. *J. Bacteriol.* 173:3559–63
39. McCutcheon JP, Agrawal RK, Philips SM, Grassucci RA, Gerchman SE, et al. 1999. Location of translational initiation factor IF3 on the small ribosomal subunit. *Proc. Natl. Acad. Sci. USA* 96:4301–6
40. Milligan RA, Unwin PN. 1986. Location of exit channel for nascent protein in 80S ribosome. *Nature* 319:693–95
41. Moazed D, Noller HF. 1987. Chloramphenicol, erythromycin, carbomycin and vernamycin B protect overlapping sites in the peptidyl transferase region of 23S ribosomal RNA. *Biochemie* 69:879–84
42. Moazed D, Noller HF. 1989. Intermediate states in the movement of transfer RNA in the ribosome. *Nature* 342:142–48
43. Moore PB, Steitz TA. 2003. After the ribosome structures: How does peptidyl transferase work? *RNA* 9:155–59
44. Morris DR, Geballe AP. 2000. Upstream open reading frames as regulators of mRNA translation. *Mol. Cell Biol.* 20:8635–42
45. Nakatogawa H, Ito K. 2002. The ribosomal exit tunnel functions as a discriminating gate. *Cell* 108:629–36
46. Nissen P, Hansen J, Ban N, Moore PB, Steitz TA. 2000. The structural basis of ribosome activity in peptide bond synthesis. *Science* 289:920–30
47. Petrelli D, Garofalo C, Lammi M, Spurio R, Pon CL, et al. 2003. Mapping the active sites of bacterial translation initiation factor IF3. *J. Mol. Biol.* 331:541–56

48. Pioletti M, Schluenzen F, Harms J, Zarivach R, Gluehmann M, et al. 2001. Crystal structures of complexes of the small ribosomal subunit with tetracycline, edeine and IF3. *EMBO J.* 20:1829–39
49. Polacek N, Gomez MJ, Ito K, Xiong L, Nakamura Y, Mankin A. 2003. The critical role of the universally conserved A2602 of 23S ribosomal RNA in the release of the nascent peptide during translation termination. *Mol. Cell* 11:103–12
50. Porse BT, Kirillov SV, Awayez MJ, Ottenheijm HC, Garrett RA. 1999. Direct crosslinking of the antitumor antibiotic sparsomycin, and its derivatives, to A2602 in the peptidyl transferase center of 23S-like rRNA within ribosome-tRNA complexes. *Proc. Natl. Acad. Sci. USA* 96: 9003–8
51. Ramakrishnan V. 2002. Ribosome structure and the mechanism of translation. *Cell* 108:557–72
52. Rodnina MV, Wintermeyer W. 2001. Ribosome fidelity: tRNA discrimination, proofreading and induced fit. *Trends Biochem. Sci.* 26:124–30
53. Rodriguez-Fonseca C, Amils R, Garrett RA. 1995. Fine structure of the peptidyl transferase centre on 23 S-like rRNAs deduced from chemical probing of antibiotic-ribosome complexes. *J. Mol. Biol.* 247:224–35
54. Sabatini DD, Blobel G. 1970. Controlled proteolysis of nascent polypeptides in rat liver cell fractions. II. Location of the polypeptides in rough microsomes. *J. Cell Biol.* 45:146–57
55. Sarker S, Rudd KE, Oliver D. 2000. Revised translation start site for secM defines an atypical signal peptide that regulates *Escherichia coli* secA expression. *J. Bacteriol.* 182:5592–95
56. Schluenzen F, Harms JM, Franceschi F, Hansen HA, Bartels H, et al. 2003. Structural basis for the antibiotic activity of ketolides and azalides. *Structure* 11:329–38
57. Schluenzen F, Tocilj A, Zarivach R, Harms J, Gluehmann M, et al. 2000. Structure of functionally activated small ribosomal subunit at 3.3 angstroms resolution. *Cell* 102:615–23
58. Schluenzen F, Zarivach R, Harms J, Bashan A, Tocilj A, et al. 2001. Structural basis for the interaction of antibiotics with the peptidyl transferase centre in eubacteria. *Nature* 413:814–21
59. Schmeing TM, Seila AC, Hansen JL, Freeborn B, Soukup JK, et al. 2002. A pre-translocational intermediate in protein synthesis observed in crystals of enzymatically active 50S subunits. *Nat. Struct. Biol.* 9:225–30
60. Shaw WV, Leslie AG. 1991. Chloramphenicol acetyltransferase. *Annu. Rev. Biophys. Biophys. Chem.* 20:363–86
61. Shevack A, Gewitz HS, Hennemann B, Yonath A, Wittmann HG. 1985. Characterization and crystallization of ribosomal particles from *Halobacterium marismortui*. *FEBS Lett.* 184:68–71
62. Spahn CM, Prescott CD. 1996. Throwing a spanner in the works: antibiotics and the translation apparatus. *J. Mol. Med.* 74:423–39
63. Srivastava S, Verschoor A, Frank J. 1992. Eukaryotic initiation factor 3 does not prevent association through physical blockage of the ribosomal subunit-subunit interface. *J. Mol. Biol.* 226:301–4
64. Stark H, Mueller F, Orlova EV, Schatz M, Dube P, et al. 1995. The 70S *Escherichia coli* ribosome at 23 Å resolution: fitting the ribosomal RNA. *Structure* 3:815–21
65. Stark H, Orlova EV, Rinke-Appel J, Junke N, Mueller F, et al. 1997. Arrangement of tRNAs in pre- and posttranslocational ribosomes revealed by electron cryomicroscopy. *Cell* 88:19–28
66. Stroud RM, Walter P. 1999. Signal sequence recognition and protein targeting. *Curr. Opin. Struct. Biol.* 9:754–59
67. Tan GT, DeBlasio A, Mankin AS. 1996. Mutations in the peptidyl transferase center of 23 S rRNA reveal the site of action of sparsomycin, a universal inhibitor of translation. *J. Mol. Biol.* 261:222–30

68. Tenson T, Ehrenberg M. 2002. Regulatory nascent peptides in the ribosomal tunnel. *Cell* 108:591–94
69. Traut RR, Monro RE. 1964. The puromycin reaction and its relationship to protein synthesis. *J. Mol. Biol.* 10:63–72
70. Unge J, Berg A, Al-Kharadaghi S, Nikulin A, Nikonov S, et al. 1998. The crystal structure of ribosomal protein L22 from *Thermus thermophilus*: insights into the mechanism of erythromycin resistance. *Structure* 6:1577–86
71. Valle M, Zavialov A, Li W, Stagg SM, Sengupta J, et al. 2003. Incorporation of aminoacyl-tRNA into the ribosome as seen by cryo-electron microscopy. *Nat. Struct. Biol.* 10:899–906
72. Vester B, Douthwaite S. 2001. Macrolide resistance conferred by base substitutions in 23S rRNA. *Antimicrob. Agents Chemother.* 45:1–12
73. Vester B, Garrett RA. 1988. The importance of highly conserved nucleotides in the binding region of chloramphenicol at the peptidyl transfer centre of *Escherichia coli* 23S ribosomal RNA. *EMBO J.* 7:3577–87
74. von Bohlen K, Makowski I, Hansen HA, Bartels H, Berkovitch-Yellin Z, et al. 1991. Characterization and preliminary attempts for derivatization of crystals of large ribosomal subunits from *Haloarcula marismortui* diffracting to 3 Å resolution. *J. Mol. Biol.* 222:11–15
75. Weisblum B. 1995. Erythromycin resistance by ribosome modification. *Antimicrob. Agents Chemother.* 39:577–85
76. Deleted in proof
77. Wilson KS, Noller HF. 1998. Molecular movement inside the translational engine. *Cell* 92:337–49
78. Wimberly BT, Brodersen DE, Clemons WM Jr, Morgan-Warren RJ, Carter AP, et al. 2000. Structure of the 30S ribosomal subunit. *Nature* 407:327–39
79. Yonath A. 2002. The search and its outcome: high-resolution structures of ribosomal particles from mesophilic, thermophilic, and halophilic bacteria at various functional states. *Annu. Rev. Biophys. Biomol. Struct.* 31:257–73
80. Yonath A. 2003. Structural insight into functional aspects of ribosomal RNA targeting. *ChemBioChem* 4:1008–17
81. Yonath A. 2003. Ribosomal tolerance and peptide bond formation. *Biol. Chem.* 384:1411–19
82. Yonath A, Glotz C, Gewitz HS, Bartels KS, von Bohlen K, et al. 1988. Characterization of crystals of small ribosomal subunits. *J. Mol. Biol.* 203:831–34
83. Yonath A, Leonard KR, Wittmann HG. 1987. A tunnel in the large ribosomal subunit revealed by three-dimensional image reconstruction. *Science* 236:813–16
84. Yonath A, Muessig J, Tesche B, Lorenz S, Erdmann VA, Wittmann HG. 1980. Crystallization of the large ribosomal subunit from *B. stearothermophilus*. *Biochem. Int.* 1:315–428
85. Yusupov MM, Yusupova GZ, Baucom A, Lieberman K, Earnest TN, et al. 2001. Crystal structure of the ribosome at 5.5 Å resolution. *Science* 292:883–96
86. Zarivach R, Bashan A, Berisio R, Harms J, Auerbach T, et al. 2004. Functional aspects of ribosomal architecture: symmetry, chirality and regulation. *J. Phys. Org. Chem.* 17:1–11
87. Woolhead CA, McCormick PJ, Johnson AE. 2004. Nascent membrane and secretory proteins differ in FRET-detected folding far inside the ribosome and in their exposure to ribosomal proteins. *Cell* 116:725–36

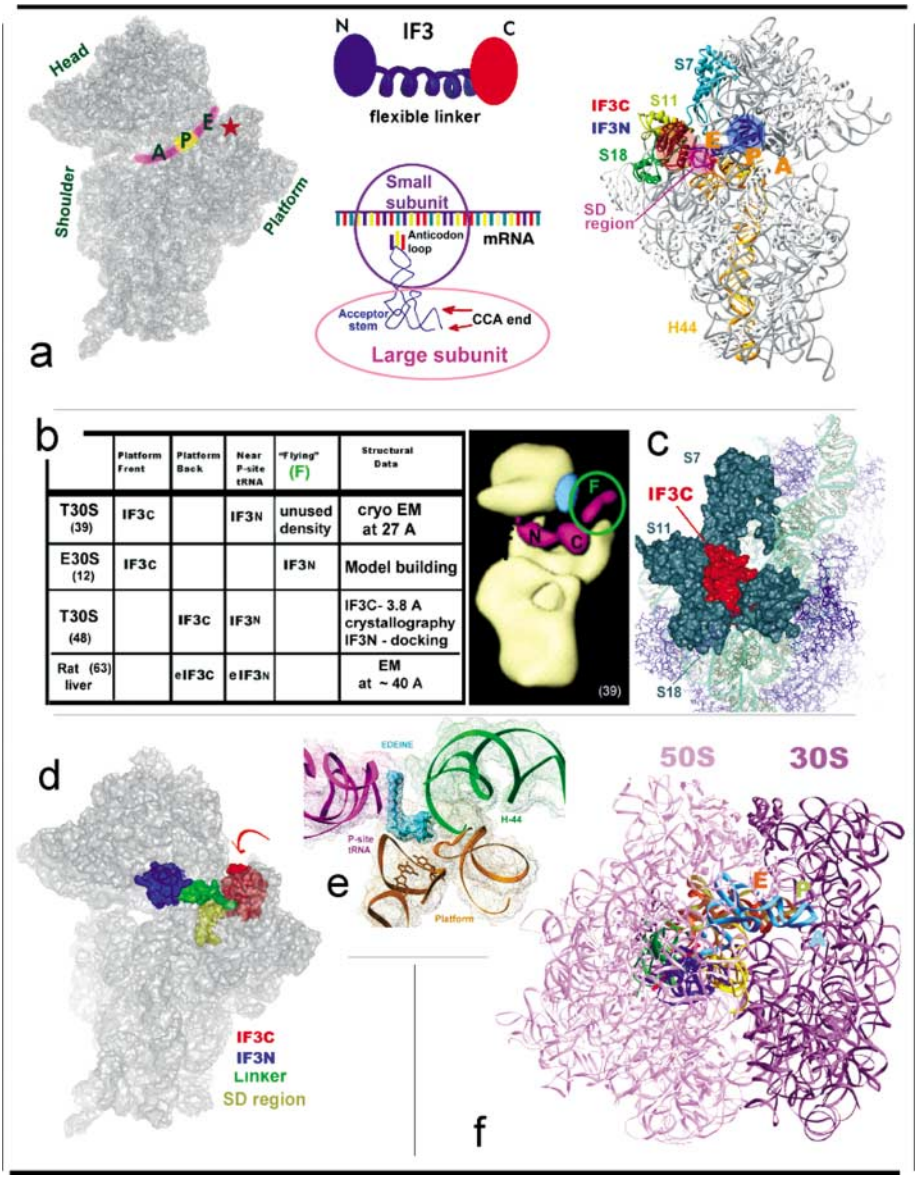

See legend on next page

Figure 1 (*a*) Left: Space-filling representation of the interface view of T30S (57), with approximate locations of the mRNA chain (*magenta*); the three tRNA molecules; the swung anti-SD region (*yellow*), serving as an mRNA analog (78); and the IF3C (*dark-red star*). Right: Ribbon representation of the solvent side of T30S highlighting the crystallographically determined (48) positions of IF3C, its neighboring proteins, the anti-SD region, and the docked IF3N. Middle: The top insert is a cartoon representing the IF3 structure. The bottom insert is a schematic representation of the tRNA structure and its location within the ribosome. (*b*) A table showing the various observed locations of IF3, and an image based on the cryo-EM structure of T30S in complex with IF3 (39). (*c*) A close-up view of the IF3C environment (48), manifesting its superb match. (*d*) Space-filling representation of the interface view of T30S with the positions of IF3C, IF3N, IF3 linker, and the SD-region. The suggested motion of IF3C is represented by the arrow. (*e*) The action of edeine. Helix H44 provides the decoding center. The tRNA molecule was docked onto T30S according to Reference 85. (*f*) The location of the three tRNA molecules within the 70S ribosome, docked on the structure of D50S, as in (*e*). The PTC in the large subunit is colored blue (A-site) and green (P-site), with tRNA 3′-end analogs in both placed according to Reference 5. Note the strategic position of bridge B2a (*yellow*), combining the two active sites and interacting with the acceptor stems of both A- and P-site tRNA. The axis of the symmetry-related region, discussed below and in References 1 and 5, is shown in red.

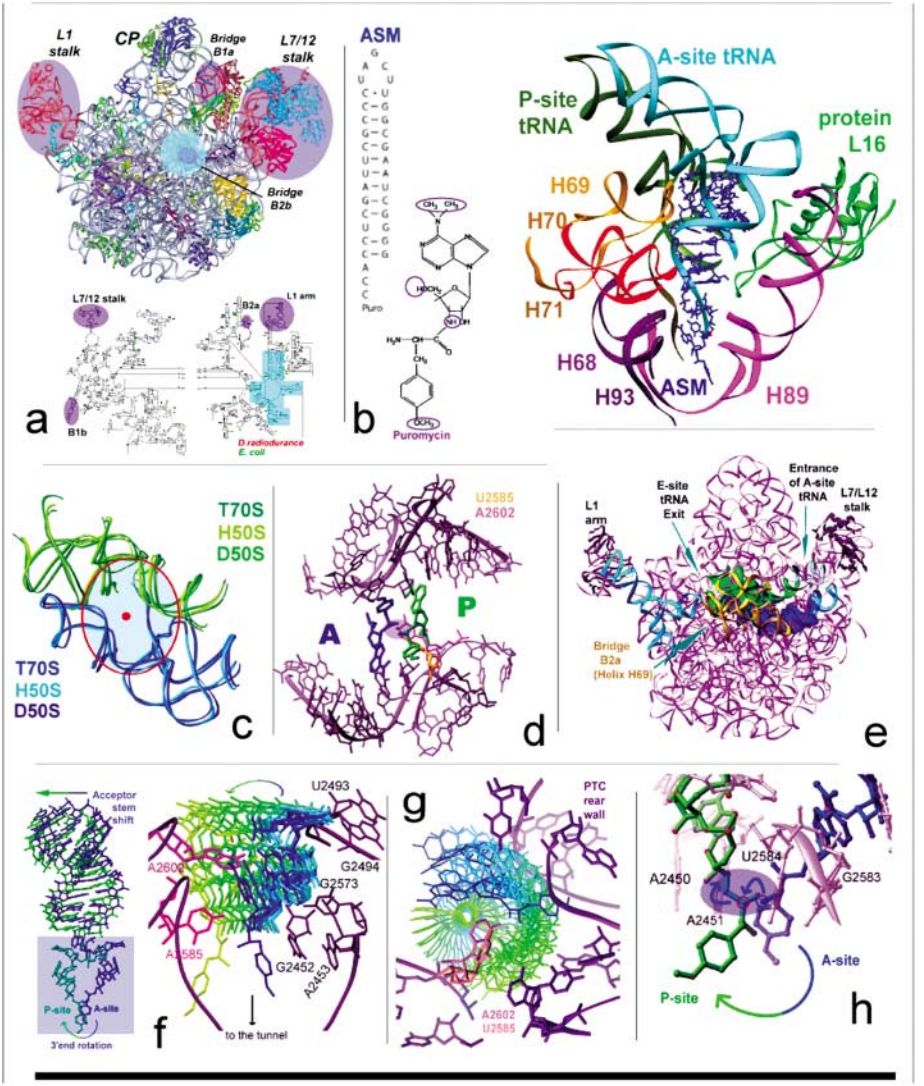

See legend on next page

Figure 2 (*a*) Top: Ribbon representation of the interface view of D50S (28). The backbone of the RNA is shown in blue, and the proteins main chains are in different colors. Purple regions designate highly flexible, functionally relevant regions that can readily become disordered, as observed in the crystal structure of H50S (4, 46). The cyan circle designates the symmetry-related region inner portion. Bottom: The 23S RNA two-dimensional diagram. The colored regions match the colored portion of the three-dimensional structure shown on top. The symmetry-related region is colored in cyan. (*b*) A side view of the PTC as in the complex of D50S with ASM (5) and the docked A-site and P-site tRNAs (85). Note the immense interaction net of helix H69 and protein L16 with ASM and A-site tRNA. The chemical compositions of ASM and the puromycin are shown on the left side. (*c–h*) The unified rotatory mechanism. The RNA backbone is purple, and blue and green represent the A-site and P-site regions, respectively, as well as the ASM and the derived P-site mimic. (*c*) The RNA backbone of the symmetry-related region as observed in all known structures, with the center of symmetry region in red. The core of the twofold symmetry-related region, including the PTC (*pale cyan*), is circled in red. The PTC and its immediate environment are circled in red. (*d*) The region circled in red in (*c*) showing nucleotides A2602 and U2585 and the approximate positions of the A-site and P-site within the PTC. (*e*) The symmetry-related region in the large subunit and its functional extensions bridging remote ribosomal functional sites (*gold and pink*). Bridge B2a, connecting the PTC with the decoding site in the small subunit, is shown in yellow. (*f–h*) The A-site to P-site passage, shown as an assembly of snapshots of the spiral motion, obtained by successive rotations from A-site to P-site of the rotating moiety shown as a gradual transition from blue to green. The blue-green turning arrows show the rotation direction. (*f*) Left: The initial and final points of tRNA translocation on the large subunit, showing the stem shift and the 3′ end (*shaded in blue*) rotating moiety. Right: The simulated rotatory motion seen perpendicular to the rotation axis. (*g*) Same as in (*f*) right, but as seen from the tunnel toward the PTC. (*h*) A representation of the formation of the peptide bond.

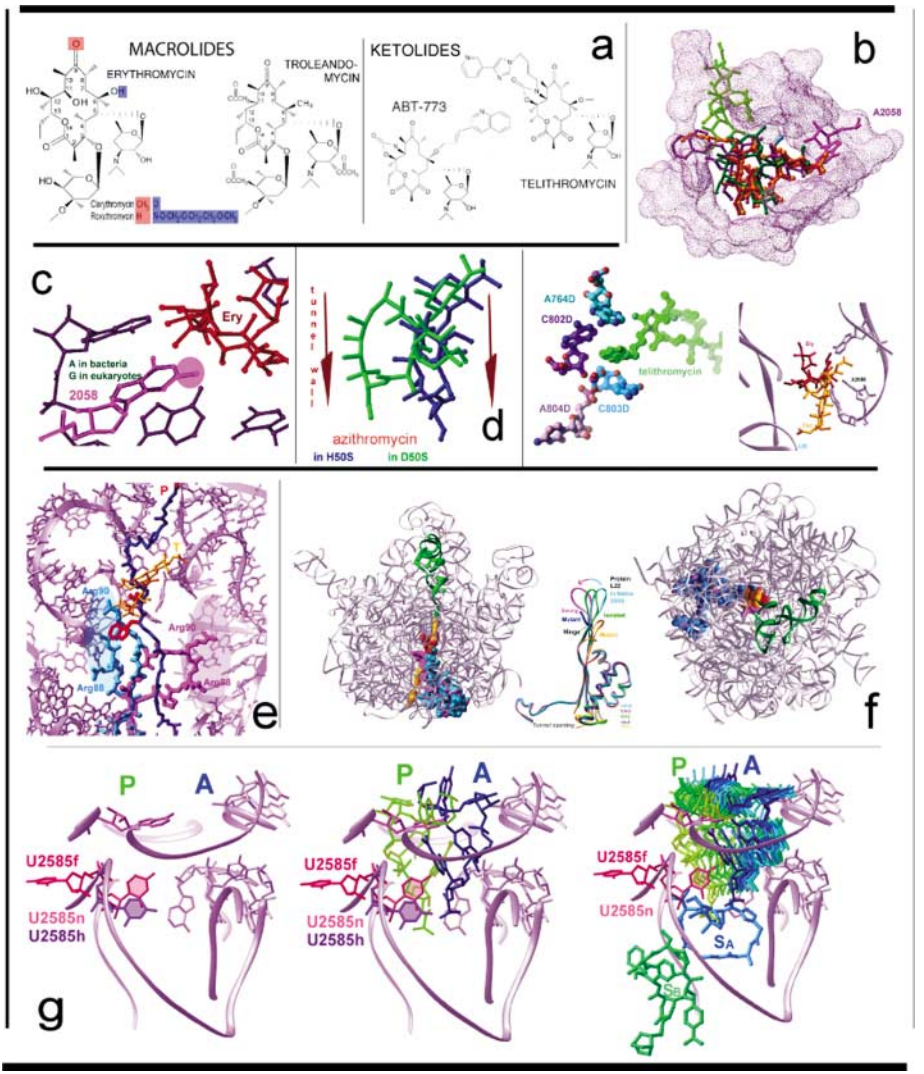

See legend on next page

Figure 3 Large subunit antibiotics and ribosomal involvement in cellular regulation. (*a*) Chemical formulas of the macrolides and ketolides shown in (*a–f*). (*b*) Various macrolide binding modes to D50S. Top: A section of the D50S ribosomal tunnel at the vicinity of macrolides-ketolides binding height. rRNA is purple, and various macrolides and ketolides bound to it (3, 7, 8, 27, 56, 58) are different colors. Nucleotide 2058 is highlighted. Bottom: The additional contacts made by telithromycin (*left*) and the special binding mode of troleandomycin (*right*). (*c*) The structural basis to macrolide selectivity based on the identity of the nucleotide in position 2058. The region leading to short contacts is highlighted in pink. (*d*) The difference in azithromycin binding to eubacterial (D50S) and archaeon (H50S) ribosomes. Note that the latter provides only limited tunnel blockage. (*e*) L22 swinging induced by troleandomycin (*gold*) binding together with a modeled nascent poly-alanine (*blue*), on which the positions of the two key residues for SecM arrest, Pro and Trp, are in red. The native L22 conformation is cyan, the swung conformation is magenta, and the ribosome RNA components are purple. The cyan- and purple-shaded areas correspond to the regions containing the mutations that bypass the elongation arrest of SecM protein (45) in L22 and in the 23S RNA, respectively. (*f*) Front and top views of D50S with P-site tRNA (*green*), the native (*cyan*) and the swung (*magenta*) L22 conformations, a modeled poly-alanine (*gold*), and the crystallographically determined position of troleandomycin (*red*). Middle: All known conformations of protein L22. Note the similarity of these structures, except for the tip of the hairpin region. (*g*) U2585 native conformation in D50S (U2585n) and its alterations induced by binding the synergetic streptogramin Synercid© (27), called U2582f. For comparison, the minor swing triggered by virginamycin M (the S_A streptogramin component) to H50S (25), U2585h, is shown. Left: The relevant PTC region. Middle: The relevant PTC region together with the A-site and P-site 3′ ends. Right: Same as middle panel but with the entire simulated A-site to P-site passage (see Figure 2*f*) and both Synercid components.